European Polymer Journal 142 (2021) 110133

Contents lists available at ScienceDirect

European Polymer Journal

journal homepage: www.elsevier.com/locate/europolj

Polymerization mechanism of 1,3-benzoxazine catalyzed by PCl_5 and rearrangement of chemical structures

Shuai Zhang [a,b], Qichao Ran [a,*], Yi Gu [a]

[a] College of Polymer Science and Engineering, Sichuan University, State Key Laboratory of Polymer Materials Engineering, Chengdu 610065, China
[b] School of Energy Science and Engineering, University of Electronic Science and Technology of China, 2006 Xiyuan Avenue, West High-Tech Zone, Chengdu, Sichuan 611731, China

ARTICLE INFO

Keywords:
Benzoxazine
PCl_5
Polymerization mechanism
Chemical structure rearrangement

ABSTRACT

Ring-opening polymerization of benzoxazine monomers is a complex process and various chemical structures including N,O-acetal structures, phenolic Mannich structures and arylamine Mannich structures are formed in polybenzoxazines. To understand the polymerization mechanism, the effects of temperature, time and solvent polarity on the polymerization routes, chemical structures and thermal properties were studied. It was discovered that the N,O-acetal structures and the phenoxy structures can be obtained in a low-polarity solvent like dichloromethane at low temperature (−20 °C) with the aid of PCl_5, while the arylamine Mannich structures can be readily generated in polar solvent like *N*,*N*-Dimethylformamide at high temperature (>80 °C) in the presence of PCl_5. However, the phenolic Mannich structures can be directly formed at high temperature (>180 °C) without any catalysts. Upon prolonging the reaction time or elevating the temperature, the phenoxy structures easily rearranged into the N,O-acetal structures or the arylamine Mannich structures. Further increasing the temperature will cause the arylamine Mannich structures to rearrange into the phenolic Mannich structures and even the phenolic methylene structures. Therefore, both phenoxy structures and N,O-acetal structures showed poor thermal stability; while the arylamine Mannich structures possessed lower initial decomposition temperature but higher char yield compared with the phenolic Mannich structures because of the formation of thermally unstable iminium ions and the anchoring of dangling aniline moieties.

1. Introduction

Polybenzoxazines (PBzs) are formed by the ring-opening polymerization (ROP) of nitrogen and oxygen containing six-membered heterocyclic compounds, 3,4-dihydro-2H-1,3-benzoxazines. They are labeled as a kind of new high-performance thermosetting resins that possess good properties similar to or even higher than phenolic resins and satisfactory processability resembling epoxy resins [1–6]. Polybenzoxazines have aroused high research enthusiasm in academic communities and drawn much attention from industries because of their well-known merits: high strength, high modulus, good thermal stability, flame retardance, good dielectric properties, good dimensional stability, low water uptake, outstanding processability and tremendous design flexibility [7–12]. More recently, polybenzoxaiznes have found many functional applications such as shape memory, self-healing, catalyst support, pollution treatment, super capacitor, CO_2 absorption and corrosion prevention [13–19]. Additionally, polybenzoxazines are of great potential in the future application as the fossil resources are decreasing rapidly but the amines and phenols that can be used to synthesize benzoxazine monomers are abundant and reproducible in nature [20–24].

Benzoxazine monomers can undergo ROP without any catalysts or curing agents. However, for benzoxazine monomers without any functional groups, due to their high activation energy of ROP, high curing temperature (>200 °C) and long curing time [25–27] are typically needed to ensure high monomer conversion and curing degree, which is critical to the mechanical and thermal properties of the resultant polybenzoxazines. Hence, developing efficient catalysts that can lower the curing temperature and shorten the curing time is of great importance in research and practical application, and many research works are focusing on addressing this issue [28–31].

ROP mechanism of benzoxazine is very complex. Theoretically, the structures including N,O-acetal structures, phenolic Mannich structures, arylamine Mannich structures and even phenolic methylene structures

* Corresponding author.
E-mail addresses: brucezhang.scu@foxmail.com (S. Zhang), ranqichao@scu.edu.cn (Q. Ran), guyi@scu.edu.cn (Y. Gu).

https://doi.org/10.1016/j.eurpolymj.2020.110133
Received 18 October 2020; Accepted 3 November 2020
Available online 12 November 2020

can be formed in the final polybenzoxazines. In reality, various catalysts, monomers and curing conditions will make the ROP process more uncontrollable and unpredictable [29–35]. Taking the catalytic ROP of an aromatic amine based benzoxazine as an example, theoretically, the ring-opening of oxazine rings can generate three cationic active intermediates, and subsequent electrophilic attack towards N atoms, O atoms, phenolic benzene rings or arylamine benzene rings would produce twelve different chemical structures (Scheme 1) [35]. Hence polybenzoxazines are always mixtures of various chemical structures, and their properties may be quite different though they are generated from the same starting monomer [14,36]. Therefore, it is a very challenging and meaningful work to study and control the ROP path of benzoxazines, and if possible, to synthesize polybenzoxazines with relatively unitary chemical structures so as to further understand the structure–property relations in polybenzoxazines.

In this report, three benzoxazine monomers without extra reactive functional groups were chosen as objects of investigation, phosphorus pentachloride (PCl_5) was used as the catalyst because of its high catalytic efficiency, dichloromethane (DCM) and *N,N*-dimethylformamide (DMF) were chosen as reaction mediums. The effects of the reaction time, temperature and solvent polarity on the chemical structures and thermal properties of the polybenzoxaiznes were systematically studied. Polybenzoxaiznes that were mainly consisted of N,O-acetal structures, phenolic Mannich structures, arylamine Mannich structures were separately obtained and their main chain rearrangement upon increasing temperature was investigated.

2. Experimental

2.1. Materials

Highly pure benzoxazine monomers, *p*C-a, *p*C-c and BA-a, were synthesized in our laboratory following the reported procedure [37–39].

*p*C-a: FTIR (KBr, cm^{-1}): 1497 (tri-substituted benzene ring skeleton stretching), 1228 (Ar-O-CH_2), 948 (benzoxazine ring), 815 (C—H stretching of tri-substituted benzene ring), 756 and 695 (C—H stretching of mono-substituted benzene ring); ^{1}H NMR (DMSO-d_6, 400 MHz, ppm) of *p*C-a: 7.50–6.50 (Ar-H), 5.40 (O-CH_2-N), 4.60 (O-CH_2-Ar), 2.19 (—CH_3).

*p*C-c: FTIR (KBr, cm^{-1}): 1501 (tri-substituted benzene ring skeleton stretching), 1225 (Ar-O-CH_2), 934 (benzoxazine ring), 813 (C—H stretching of tri-substituted benzene ring); ^{1}H NMR (DMSO-d_6, 400 MHz, ppm) of *p*C-a: 7.50–6.50 (Ar-H), 4.87 (O-CH_2-N), 3.96 (O-CH_2-Ar), 2.17 (—CH_3), 2.60–1.04 (H in cyclohexyl).

BA-a: FTIR (KBr, cm^{-1}): 1496 (tri-substituted benzene ring skeleton stretching), 1233 (Ar-O-CH_2), 947 (benzoxazine ring), 822 (C—H stretching of tri-substituted benzene ring), 756 and 695 (C—H stretching of mono-substituted benzene ring); ^{1}H NMR (DMSO-d_6, 400 MHz, ppm): 7.50–6.50 (Ar-H), 5.39 (O-CH_2-N), 4.60 (O-CH_2-Ar), 1.53 (—CH_3).

Analytical grade dichloromethane (DCM) and *N,N*-dimethylformamide (DMF) was purchased from Chengdu Kelong Chemical Reagents Co., Ltd (Chengdu China) and used as received. Phosphorus pentachloride (PCl_5) were purchased from Adamas Reagent Co., Ltd (Shanghai China).

2.2. ROP of benzoxazines

2.2.1. Phenolic Mannich polybenzoxazines prepared by thermally induced ROP

Appropriate amount of *p*C-a and *p*C-c were placed in an air-circulating oven and cured at 160 °C, 180 °C, 200 °C and 220 °C for 1 h, respectively. After each curing stage, the samples were taken out and cooled slowly to room temperature. The sample of curing *p*C-a at 160 °C was labeled as P*p*C-a@160 and others were named the same way.

2.2.2. N,O-acetal and phenoxy type polybenzoxazines prepared by catalytic ROP of pC-a and pC-c in DCM

Appropriate amount of *p*C-a or *p*C-c and 2 wt% PCl_5 were dissolved in DCM to give transparent solutions with a resin content of 20 wt%. The solutions were then placed in thermostats without stirring at −20 °C and 30 °C for 24 h, respectively. In order to evaluate the influence of the reaction time, catalytic ROP of *p*C-a at 30 °C for 96 h (4 days) was also carried out. After desired time, a small amount of solution was coated onto a glass slide and the solvent was removed by high vacuo for about 10 min, and the characterizations were performed immediately. Here polybenzoxazines synthesized from *p*C-a at −20 °C and 30 °C for 24 h were named as *p*C-a/P@-20 and *p*C-a/P@30, respectively. The one synthesized at 30 °C for 4 days was named as *p*C-a/P@30-4D. Polybenzoxazines synthesized from *p*C-c were named as *p*C-c/P@-20 and *p*C-c/P@30, respectively, according to the reaction temperature.

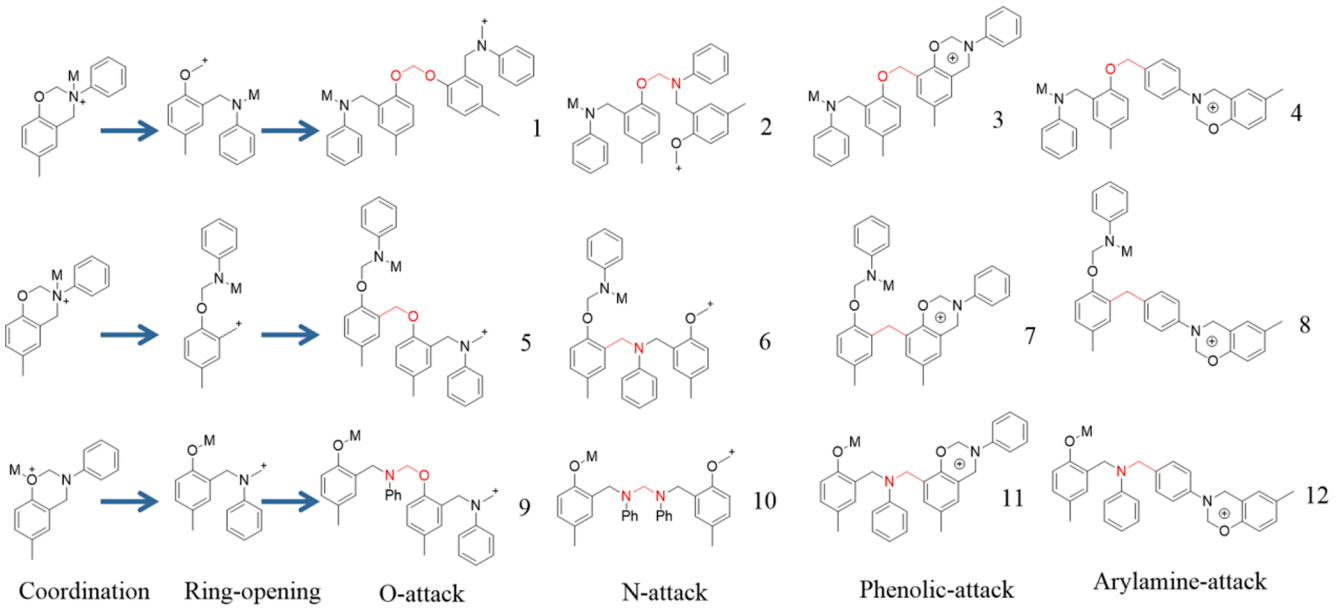

Scheme 1. All possible chemical structures of the products from the first step ROP of benzoxazine initiated by Lewis acids.

2.2.3. Arylamine Mannich polybenzoxazines prepared by catalytic ROP of pC-a in DMF

Appropriate amount of *p*C-a and 2 wt% PCl_5 were dissolved in DMF to give transparent solutions with a resin content of 20 wt%. Then the catalytic ROP of *p*C-a was performed in water bath at 80 °C. After different period of time, the samples were draw out, coated onto glass plates and placed under high vacuo to maximally remove the solvents, though the solvents cannot be completely removed as the characterization revealed. After reaction for 180 min, the solution was coated onto a glass slide and the solvent was removed by high vacuo at 100 °C for 1 h to yield a brittle, light yellow and transparent film, which was labeled as *p*C-a/P@100. To investigate the main chain rearrangement of the obtained polybenzoxazines, *p*C-a/P@100 was heated at 150 °C and 200 °C for 1 h, and the obtained samples were named as *p*C-a/P@150 and *p*C-a/P@200, respectively.

2.2.4. N,O-acetal polybenzoxazines prepared by catalytic ROP of BA-a in DCM

Appropriate amount of BA-a and 2 wt% PCl_5 were dissolved in DCM to give transparent solutions with a resin content of 20 wt%. Then the catalytic ROP of BA-a was performed in water bath at 4 °C, 15 °C and 30 °C with continuous stirring for 24 h. During the reaction process, the transparent solutions gradually turned into suspensions because the high-molecular-weight polybenzoxazines were generated and they were insoluble in DCM. After filtration and vacuum drying, brittle white films were obtained for ROP carried out at 4 °C and 15 °C, while fluffy yellow powder was obtained for ROP carried out at 30 °C (Fig. S2). The samples were named as BA-a/P@4, BA-a/P@15 and BA-a/P@30, respectively. The characterization of the samples was carried out shortly in order to avoid the change of the chemical structures.

2.3. Characterization

Differential scanning calorimetry (DSC) tests were conducted by a DSC Q20 (TA Instruments) at a heating rate of 10 °C/min under nitrogen atmosphere. Calibration was made using an indium standard, about 3 mg of samples were sealed in the aluminum pan for scanning. Fourier transform infrared (FTIR) spectra were obtained with a Nicolet-560 spectrometer in the range of 4000–400 cm^{-1} at a resolution of 4 cm^{-1}. Powder samples were mixed with spectroscopy grade KBr to make pellets. Molecular weight was estimated by size exclusion chromatography (SEC) on a Tosoh HLC-8320 system equipped with two consecutive polystyrene gel columns (TSKgel Super HZM-M 6 × 150 mm and TSKgel Super HZ3000 6 × 150 mm) and a refractive index (RI) detector at a flow rate of 0.6 mL/min. DMF was chosen as eluent, and polystyrene as calibration standards. Thermal gravimetric analysis (TGA) were performed on NETZSCH TG 209F1 Iris (NETZSCH Instruments), the polymer samples were heated from 35 °C to 800 °C in nitrogen atmosphere with a flow rate of 40 mL/min and a heating rate of 10 °C/min.

3. Results and discussion

3.1. Phenolic Mannich type polybenzoxazines prepared by thermally induced ROP

In most cases, polybenzoxazines are prepared by thermally induced ROP of the corresponding monomers without the presence of any catalysts or curing agents. Here *p*C-a and *p*C-c were employed as model compounds to investigate the chemical structures of the thermally cured polybenzoxazines. Their Fourier transform infrared (FTIR) and hydrogen proton nuclear magnetic (^{1}H NMR) spectra are shown in Fig. S1, and the chemical structures are shown in Scheme 2. The paracresol-based monofunctional benzoxazines were deliberately chosen for characterization convenience. Fig. 1a shows the FTIR spectra of the poly(*p*C-a)s from different curing temperatures. After curing at 160 °C for 1 h, a small broad band attributed to hydroxyl groups was

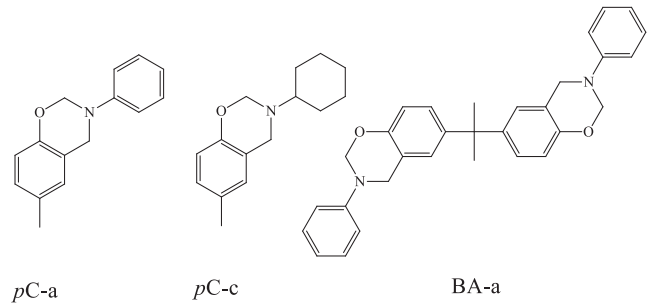

Scheme 2. Chemical structures of *p*C-a, *p*C-c and BA-a.

observed at around 3400 cm^{-1}, manifesting the ring-opening of the benzoxazine monomers and the formation of some hydroxyl groups [40]. Moreover, two weak bands showed up in the range of 1650–1680 cm^{-1}, and they disappeared after curing at 200 °C. It is speculated that these two absorption bands were attributable to carbocations and iminium ions formed by ring-opening of *p*C-a and these reactive intermediates were consumed by chain propagation at higher temperature [14,41]. The characteristic band of the oxazine ring at 947 cm^{-1} disappeared completely after curing at 180 °C, meaning the complete consumption of the monomers, which was consistent with the disappearance of signals at 5.39 and 4.60 ppm due to the CH_2 units in oxazine rings (Fig. 1d). Additionally, with the gradual fading of tri-substituted benzene ring characteristic absorption bands at 822 cm^{-1} (Ar—H stretching) and 1496 cm^{-1} (C═C stretching), the tetra-substituted benzene ring absorption band at 860 cm^{-1} (Ar—H stretching) and 1479 cm^{-1} (C═C stretching) emerged [42]. Meanwhile, the mono-substituted benzene ring absorption band at 750 cm^{-1} and 693 cm^{-1} (Ar—H stretching) kept almost intact. All these features suggested that the carbocations attacked the electron-rich *ortho*-position of phenolic hydroxyls and phenolic Mannich type polybenzoxazines were synthesized (Scheme 3). It is clearly shown that the signal of CH_2 proton in phenolic Mannich bridge structures (structure h in Scheme 3) centered at around 3.71 ppm, which is consistent with the previous report [43]. Furthermore, the signal of carbon nuclei in phenolic Mannich bridge structures (structure h) centered at around 31.65 ppm was shown in ^{13}C NMR spectra in Fig. 1b; it should be noted that the chemical shift of CH_2 carbon nuclei in polybenzoxazines is rarely reported and this is an important evidence for further structure identification. As for poly(*p*C-c) prepared by thermally induced ROP, the tetra-substituted benzene ring absorption bands at 857 cm^{-1} (Ar—H stretching) and 1481 cm^{-1} (C═C stretching) and the signal of CH_2 proton in phenolic Mannich bridge structures at around 3.74 ppm are shown in the FTIR and ^{1}H NMR spectra of P*p*C-c@200 (Fig. S3), indicating phenolic Mannich type polybenzoxazines were formed by thermally induced ROP, no matter aromatic or aliphatic amines were used to synthesize the benzoxazine monomers.

The SEC tests of the as-prepared polybenzoxazines were performed to determine the molecular weight and the polydispersity index (PDI). As shown in Table 1, the molecular weight and PDI increased with the elevated temperature; the highest M_w of 37,511 D was reached for P*p*C-a@200. Though very few monomers was consumed at 160 °C as suggested by the FTIR and ^{1}H NMR spectra of P*p*C-a@160, its M_w was 10.17 times as that of *p*C-a, hence FTIR and NMR spectra may not be that sensitive. It should be mentioned that P*p*C-a@220 wasn't completely soluble in DMF, so no molecular weight and PDI was provided, which suggested its very high molecular weight or a certain degree of crosslinking.

3.2. N,O-acetal And phenoxy type polybenzoxazines prepared by catalytic ROP of pC-a and pC-c in DCM

N,O-acetal and phenoxy type polybenzoxazines are relatively

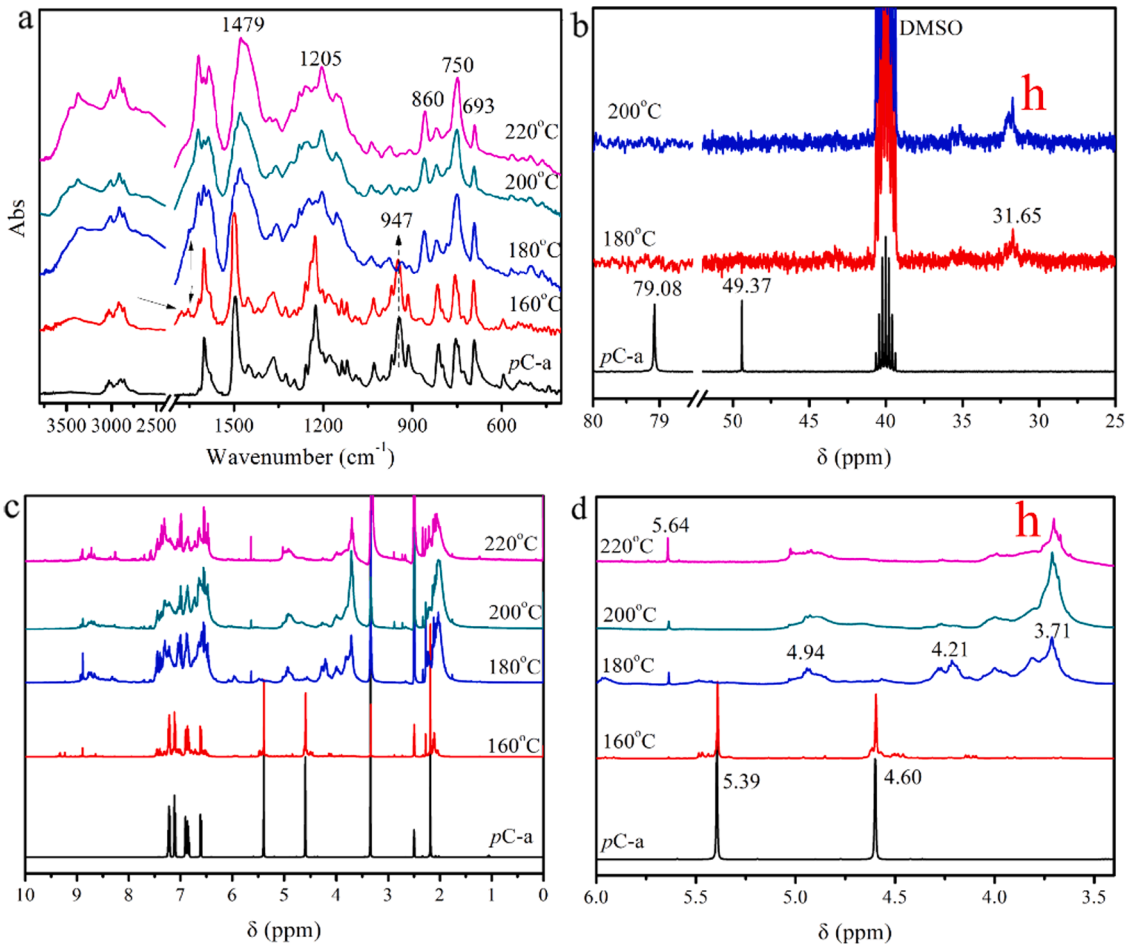

Fig. 1. FTIR spectra (a), ^{13}C NMR spectra (b) and ^{1}H NMR spectra (c, d) of poly(*p*C-a)s cured at different temperatures without catalysts.

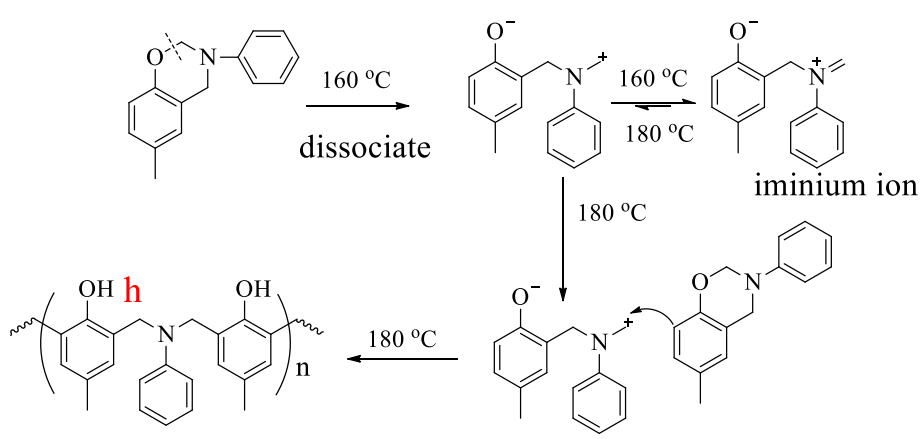

Scheme 3. Proposed reaction route for thermally induced ROP of *p*C-a.

Table 1
SEC results of *p*C-a and poly(*p*C-a)s cured at different temperatures.

Sample	*Mn* (Dalton)	*Mw* (Dalton)	PDI
*p*C-a	472	487	1.03
P*p*C-a@160	4802	5461	1.14
P*p*C-a@180	14,834	23,571	1.59
P*p*C-a@200	16,382	37,511	2.29

unstable and tend to rearrange into other chemical structures [44,45], hence the reaction was conducted at relatively low temperatures (−20 °C and 30 °C), and a low-polarity solvent, DCM, was used to ensure high moveability of molecules, PCl_5 was chosen as the catalyst due to its high catalytic activity. Fig. 2 presents the FTIR spectra of poly(*p*C-a)s and poly(*p*C-c)s obtained by catalytic ROP in DCM at −20 °C and 30 °C for 24 h, respectively. The FTIR spectra of the polybenzoxazines were very similar to those of the monomers, except for the broad absorption band at around 3400 cm^{-1} due to the hydroxyl groups, which meant some oxazine rings opened and phenolic hydroxyls were formed. FTIR

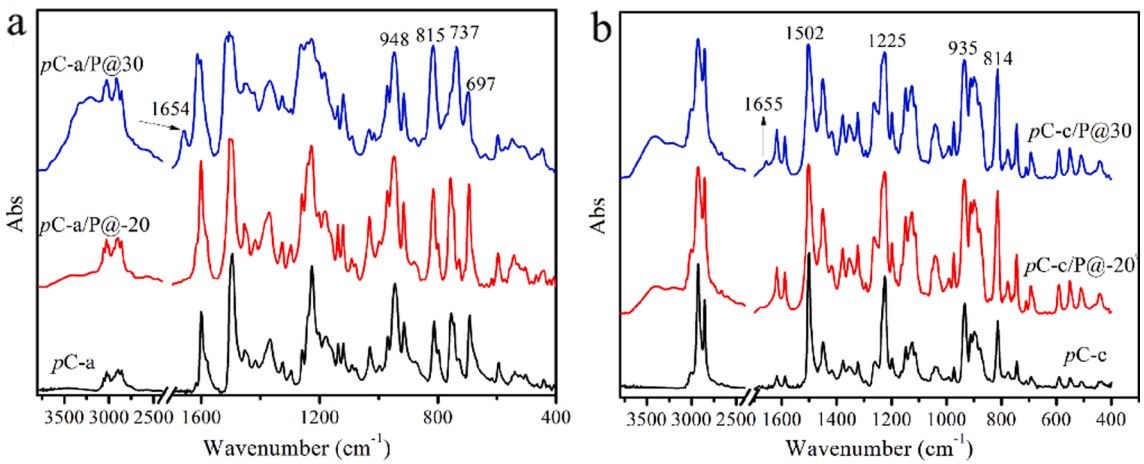

Fig. 2. FTIR spectra of poly(*p*C-a)s (a) and poly(*p*C-c)s (b) obtained by catalytic ROP at −20 °C and 30 °C for 24 h in DCM.

spectra have been proven to be inadequate to quantify monomer contents [41,42], hence the high intensities of the absorption bands at 948 cm^{-1} and 935 cm^{-1} didn't necessarily mean that massive benzoxazine monomers were remained. It is also noteworthy that the intensity of intensity of the band at around 3400 cm^{-1} seems to be compabale with that of the phenolic Mannich type P*p*C-a@200. It is believed that in P*p*C-a@200, much phenolic OH form intramolecular hydrogen bonding and the intensity of phenolic OH is flattened, while in *p*C-a/P@-20 and *p*C-a/P@30, much less intramolecular HB is formed. Such inference may be evidenced by the difference in intensity of the intramolecular hydrogen bonding (in the range of 2900–2400 cm^{-1}) in the FTIR spectra of these two types of polybenzoxazines. For *p*C-a/P@30 and *p*C-c/P@30, the absorption bands of iminium ions (1655 cm^{-1} and 1654 cm^{-1}) were higher than *p*C-a/P@-20 and *p*C-c/P@-20, meaning more active carbocations were generated at higher temperature and the unreacted carbocations remained in the form of inert iminium ions.

The ^{1}H NMR spectra were obtained to further investigate the chemical structures of the polybenzoxazines (Fig. 3). In Fig. 3a, obvious phenolic hydroxyl proton signal appeared at around 9.32 ppm for *p*C-a/P@-20 and *p*C-a/P@30, suggesting the generation of phenolic hydroxyls. Moreover, as shown in Fig. 3b, the signal of CH_2 proton in oxazine ring (structure a and b, Scheme 4) weakened significantly, while a major signal emerged at around 4.45 ppm which may be attributed to the formation of phenoxyl structures (structure e, Scheme 4).

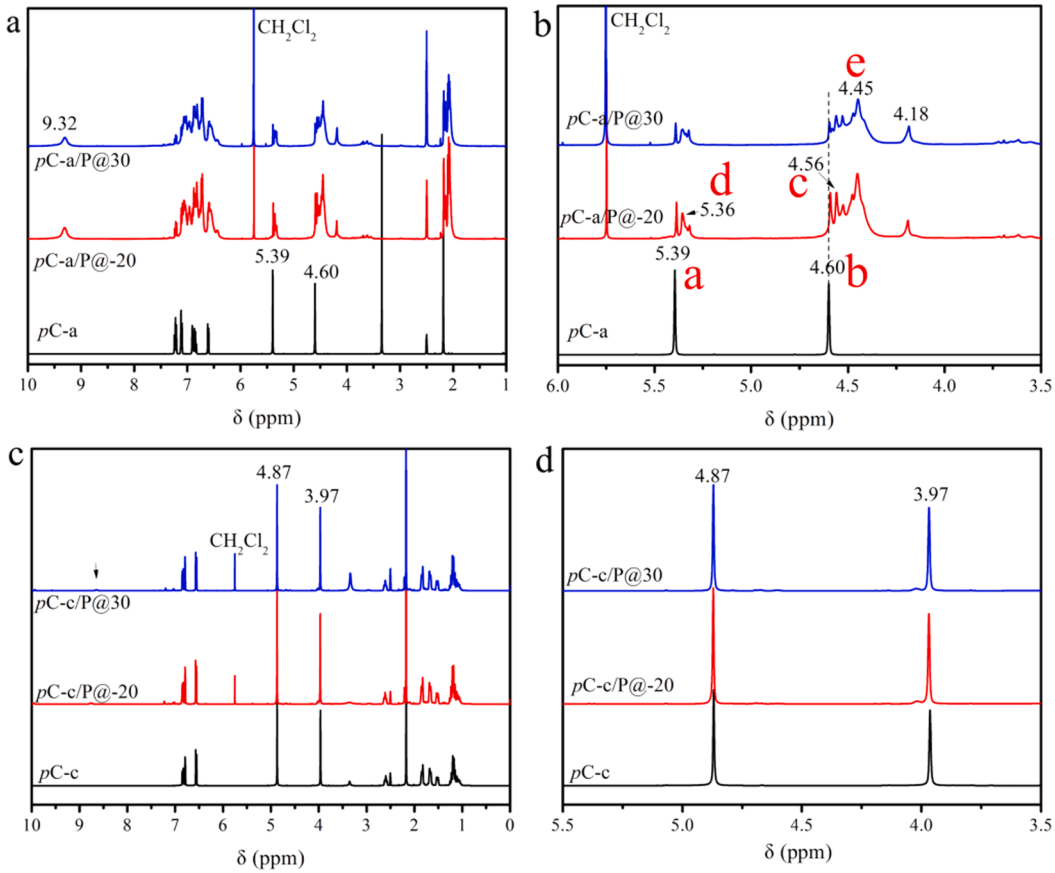

Fig. 3. ^{1}H NMR spectra of poly(*p*C-a)s (a, b) and poly(*p*C-c)s (c, d) obtained by catalytic ROP at −20 °C and 30 °C for 24 h in DCM.

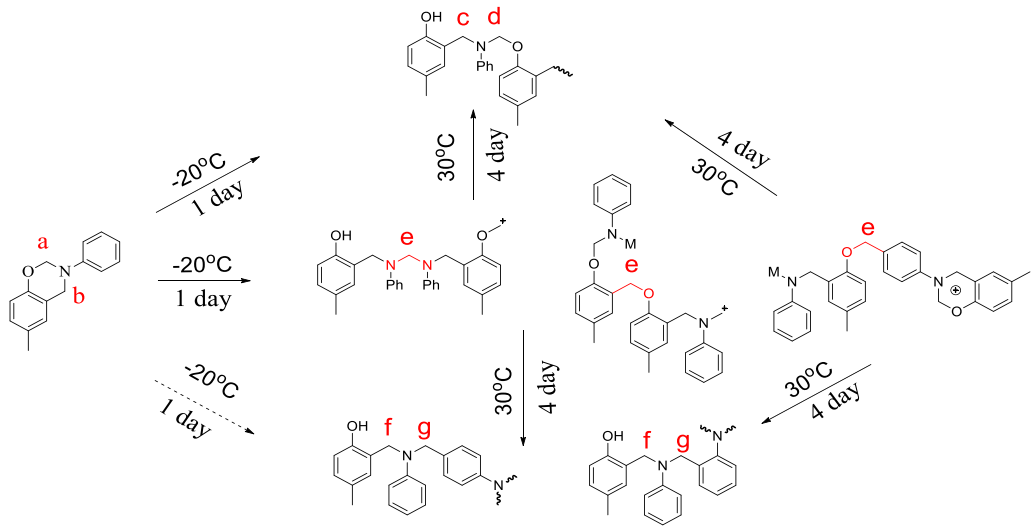

Scheme 4. Proposed ROP and transformation routes of *p*C-a in DCM at −20 °C and 30 °C for different period of time.

Additionally, some minor signals appeared at around 5.36 ppm and 4.56 ppm that were quite adjacent to the signal of CH_2 proton in oxazine ring; these signals indicated the formation of some N,O-acetal structures (structure c, d, Scheme 4) [46–48]. In short, the polybenzoxazines synthesized by catalytic ROP in DCM from *p*C-a were mainly composed of phenoxyl structures and a small portion of N,O-acetal structures. However, the polybenzoxazines synthesized from the aliphatic amine-based monomer showed some differences. As shown in Fig. 3c, d and Fig. S4, the NMR spectra of *p*C-c/P@-20 and *p*C-c/P@30 were almost identical to that of the monomer; the signal of phenolic hydroxyls at around 8.50 ppm (indicated by arrow) was almost unobservable and the signal of CH_2 proton in oxazine ring at 4.87 and 3.97 ppm seldom changed. These features suggested that no ROP happened for *p*C-c, but the M_n (Table 2) of *p*C-c/P@-20 and *p*C-c/P@30 were 8 times higher than that of *p*C-c, which was in accordance with the previous reports that the signal of CH_2 proton in N,O-acetal structures from methylamine-based benzoxazine was almost the same as the signal of the monomer [48]. Therefore, the N,O-acetal structures were easier to be obtained from aliphatic amine-based benzoxazine when compared with aromatic amine counterpart.

In order to probe the influence of the reaction time on the chemical structures, poly(*p*C-a)s synthesized by catalytic ROP of *p*C-a in DCM at 30 °C for 24 h (*p*C-a/P@30-1D) and 96 h (*p*C-a/P@30-4D) were characterized and compared. As the FTIR spectra in Fig. 4a shows, the characteristic absorption band by the oxazine ring at 947 cm^{-1} decreased with prolonged reaction time, suggesting higher conversion rate of *p*C-a. Notably, the tri-substituted benzene ring characteristic absorption bands at 815 cm^{-1} (Ar—H stretching) and 1500 cm^{-1} (C═C stretching) remained unchanged and no tetra-substituted benzene ring absorption band was present, manifesting nearly no generation of phenolic Mannich structures. Interestingly, due to more consumption of the monomer and possible chemical structure transformation, the absorption band of mono-substituted benzene ring at 754 cm^{-1} (Ar—H stretching) gradually red-shifted to 733 cm^{-1} for *p*C-a/P@30-4D. Moreover, as shown in ^{1}H NMR spectra (Fig. 4b), the signal of phenoxyl CH_2 (structure e) proton at 4.45 ppm decreased but the signals of N,O-acetal CH_2 (structure c, d) proton at 5.32 and 4.53 ppm and arylamine Mannich CH_2 (structure f, g) proton at 4.12 and 3.64 ppm increased; these characteristics suggested that phenoxyl structures were relatively unstable and would transform into N,O-acetal and arylamine Mannich structures with the prolonging of the reaction time. The ^{13}C NMR spectra (Fig. 4c) provided further evidence, as the obvious signal of carbon nuclei in phenoxyl CH_2 (structure e) disappeared and the signals of carbon nuclei in N,O-acetal CH_2 (structure c, d) dominated after reaction for 4 days. It should be noted that no other signal of methylene carbon nuclei was observed (Fig. S5) in ^{13}C NMR spectra of *p*C-a/P@30-4D, hence it is concluded that *p*C-a/P@30-4D is mainly consisted of the N,O-acetal structures. A possible ROP and transformation route of *p*C-a catalyzed by PCl_5 in DCM is proposed and shown in Scheme 4. To highlight the differences of phenolic Mannich and N,O-acetal polybenzoxazines, the FTIR spectra of P*p*C-a@220 and *p*C-a@30-4D are depicted in Fig. 4d. Clearly, they were quite different in terms of substituted benzene ring absorption bands as discussed above.

Table 2
SEC test results of poly(*p*C-a)s and poly(*p*C-c)s catalyzed by PCl_5 in DCM at −20 °C and 30 °C for 24 h.

Sample	*Mn* (Dalton)	*Mw* (Dalton)	PDI
*p*C-a	472	487	1.03
*p*C-a/P@-20	4023	4592	1.14
*p*C-a/P@30	7452	9416	1.26
*p*C-c	471	487	1.03
*p*C-c/P@-20	4219	4822	1.14
*p*C-c/P@30	4585	5273	1.15

3.3. Arylamine Mannich polybenzoxazines prepared by catalytic ROP of *p*C-a in DMF

To explore the effects of the solvent polarity and the reaction temperature on the ROP mechanism and chemical structure of the polybenzoxazines, ROP of *p*C-a was carried out in polar DMF at 80 °C. Fig. 5a presents the FTIR spectra of poly(*p*C-a)s obtained after different reaction time. The characteristic absorption band of the oxazine ring at 947 cm^{-1} decreased gradually and completely disappeared after 90 min, suggesting complete consumption of the monomers. The tri-substituted benzene ring absorption bands at 813 cm^{-1} (Ar—H stretching) and 1508 cm^{-1} (C═C stretching) remained unchanged and no tetra-substituted benzene ring absorption band was shown, nevertheless, the mono-substituted benzene ring absorption bands at 755 cm^{-1} (Ar—H stretching) disappeared after 10 min, which suggested that the active carbocations attacked the dangling aniline moieties rather than the phenolic benzene rings. Therefore, the as-prepared polybenzoxazines are mainly consisted of arylamine Mannich structures. It was also worth noting that the absorption bands of Ar—O and C—N—C stretching showed up at 1258 and 1100 cm^{-1}, respectively. Additionally, due to high reaction temperature and high polarity of the solvent, massive active intermediates like carbocations were generated and they preserved in the form of iminium ions in the final polybenzoxazines.

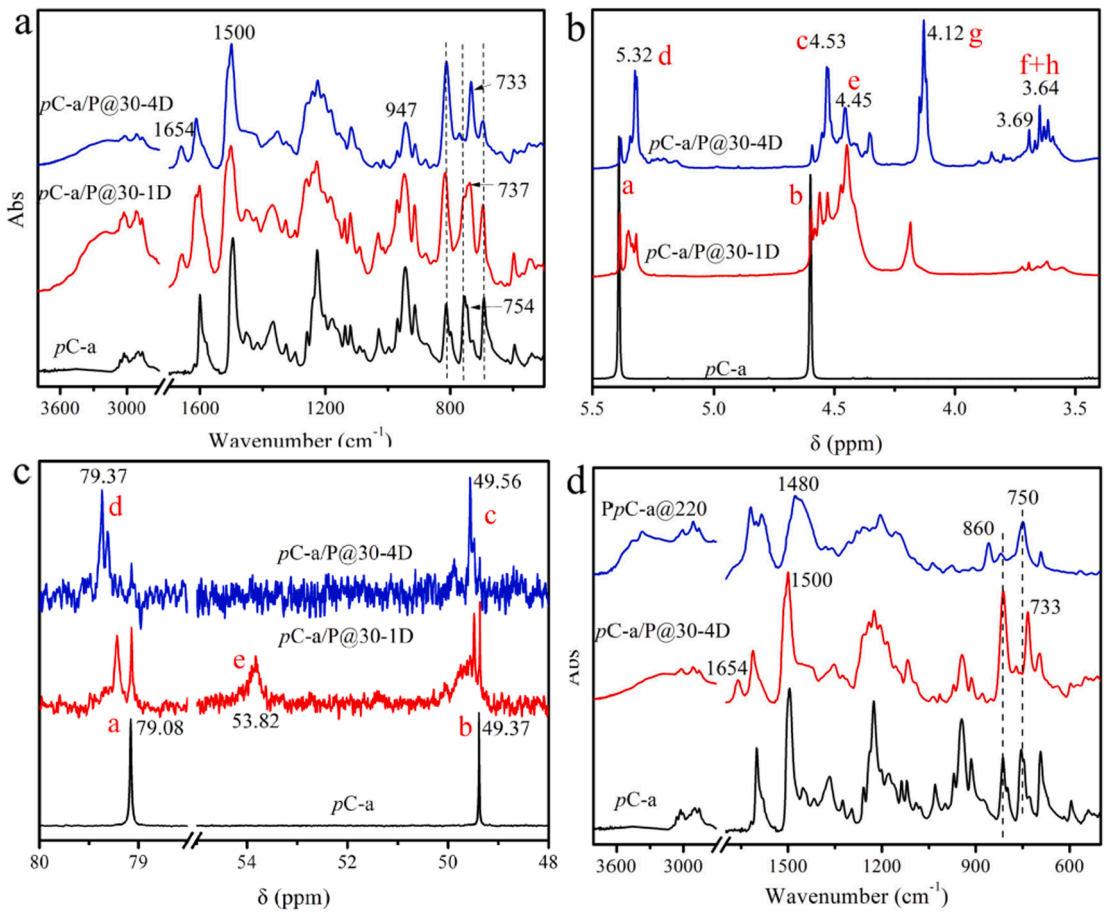

Fig. 4. FTIR spectra (a), ^{1}H NMR spectra (b) and ^{13}C NMR spectra of poly(*p*C-a)s obtained by catalytic ROP at 30 °C for different period of time in DCM, comparison of FTIR spectra (d) of P*p*C-a@220 and *p*C-a@30-4D.

Consequently, the absorption band intensity of iminium ions at 1652 cm^{-1} was high.

The ^{1}H NMR spectra in Fig. 5b and d are employed to further probe the chemical structures. The signal of CH_2 proton in the oxazine ring (structure a, b) decreased rapidly and vanished after 20 min; meanwhile, some minor signals that were attributed to N,O-acetal CH_2 proton (structure c, d) showed up at the vicinity of the original signal of CH_2 proton in the oxazine ring, which indicated the formation of N,O-acetal structures at the early stage. After reaction for 20 min, the ^{1}H NMR spectra of the products were almost the same, which was in accordance with the invariability of the SEC results (Table S1). Such features revealed that catalytic ROP of *p*C-a completed within 20 min and the chemical structures didn't change since then. Nevertheless, it is worth noting that the signals at 4.10 and 3.57 ppm attributed to arylamine Mannich CH_2 proton (structure g, f) became dominating, and the signals of N,O-acetal CH_2 proton disappeared after being further treated at 100 °C. In the ^{1}H NMR spectra of *p*C-a/P@100, the clear signal of phenoxyl structures (structure e) at around 4.45 ppm was seen. However, only the signals of arylamine Mannich CH_2 carbon nuclei were observed at 49.89 and 42.14 ppm in the ^{13}C NMR spectra of *p*C-a/P@100 (Fig. 5d and Fig. S6). Therefore, as Scheme 5 describes, the N,O-acetal structures were generated at the early stage in polar DMF at 80 °C with PCl_5, but these structures were relatively unstable and transformed to arylamine Mannich structures as the temperature rose and the reaction proceeded.

3.4. Chemical structure rearrangement of arylamine Mannich polybenzoxazines at high temperature

The chemical structure evolution of *p*C-a/P@100 at 150 °C and 200 °C in bulk state was further explored. As can be observed in the FTIR spectra (Fig. 6a), the absorption band of the iminium ion at 1654 cm^{-1} decreased significantly while a new band of tetra-substituted benzene ring emerged at 1475 cm^{-1}. Moreover, in the ^{1}H NMR spectra (Fig. 6b and c), the signal of the proton in iminium ions at 7.94 ppm gradually weakened; the signal of phenoxyl CH_2 proton at 4.46 ppm disappeared after 150 °C, and the signal of the arylamine Mannich CH_2 proton at 4.10 ppm disappeared after 200 °C [44]. Consequently, only the signal of phenolic Mannich CH_2 proton and phenolic CH_2 proton was shown at 3.62 ppm for *p*C-a/P@200. Such characteristics suggested that the iminium ions were activated and attacked the *ortho*-position of phenolic moieties, forming phenolic Mannich structures (structure h in Scheme 6). Additionally, the arylamine Mannich structures may dissociate and generate carbocations that reacted with phenolic moieties, producing phenolic methylene and phenolic Mannich methylene (structure h in Scheme 6). The ^{13}C NMR spectra in Fig. 6d further validated such chemical transformation, as new signals attributed to the phenolic methylene and phenolic Mannich CH_2 carbon nuclei showed up at 30.96 and 34.79 ppm, respectively, after post-treated at 150 °C. Moreover, the M_n decreased substantially from 8398 D to 5948 D after post-treated at 150 °C due to dissociation of molecular chain, but *p*C-a/P@200 was hardly soluable in eluent (DMF), hence its SEC result was not obatained, which may indicate further rearrangement and chain propagation at 200 °C. The ^{13}C NMR spectrum of *p*C-a/P@200 is not shown because the signal is so weak due to low solubility in DMSO. Lastly but importantly,

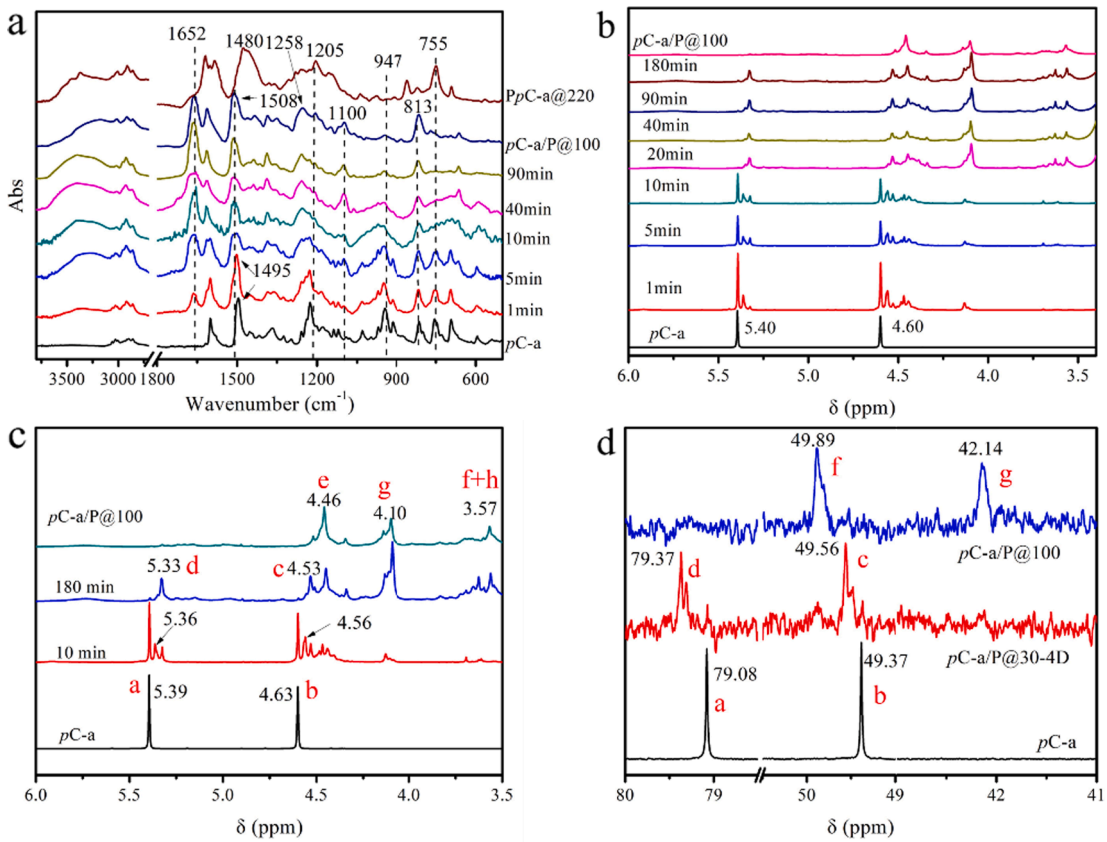

Fig. 5. FTIR spectra (a), ^{1}H NMR spectra (b, c) and ^{13}C NMR spectra (d) of poly(*p*C-a)s obtained by catalytic ROP at 80 °C for different period of time in DMF.

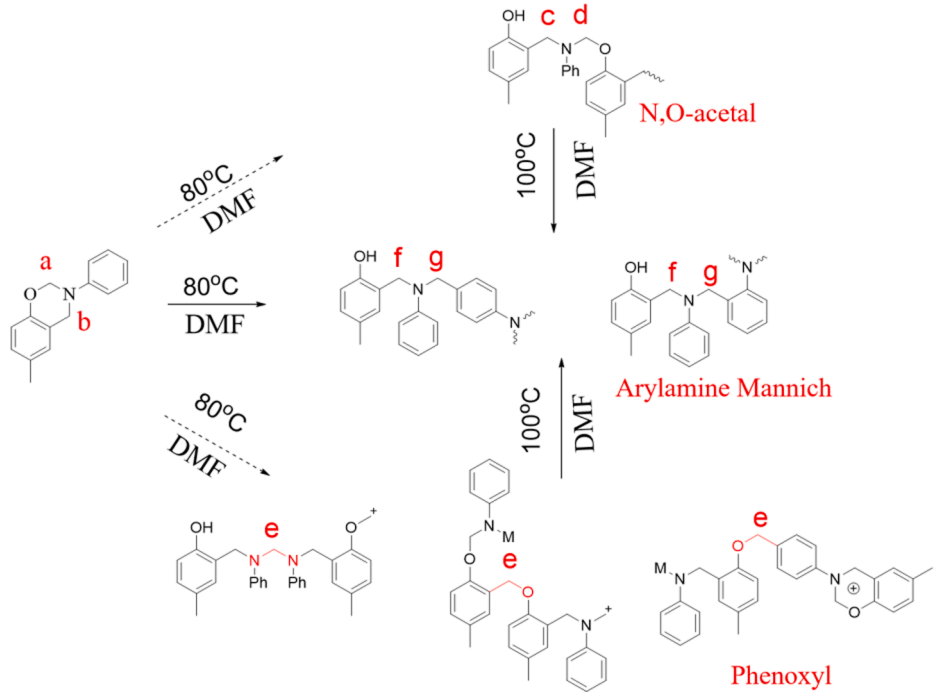

Scheme 5. Proposed ROP routes for poly(*p*C-a) catalyzed by PCl_5 in DMF.

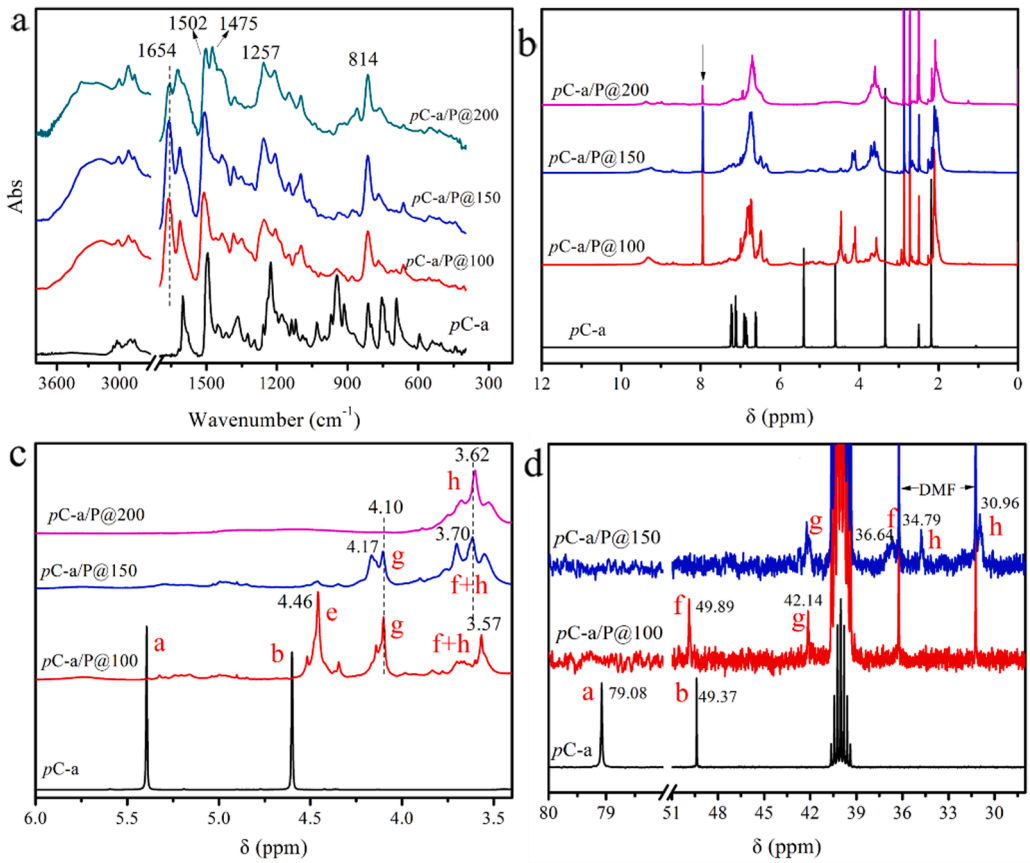

Fig. 6. FTIR spectra (a), ^{1}H NMR spectra (b, c) and ^{13}C NMR spectra (d) of *p*C-a, *p*C-a/P@100 and post-treated products at 150 and 200 °C.

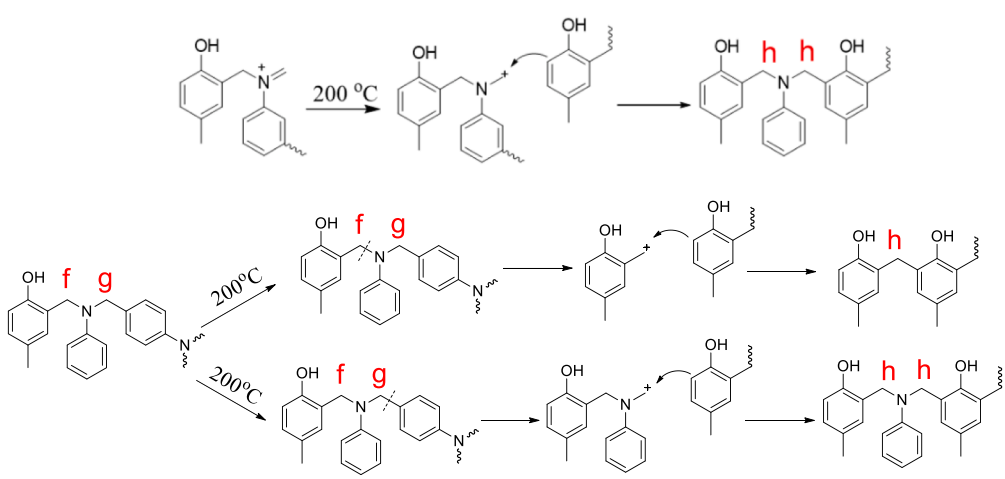

Scheme 6. Proposed structure evolution of *p*C-a/P@100 at 200 °C.

it should be emphasized that the rearrangement from arylamine Mannich structures to phenolic and phenolic Mannich structures may not be thorough and *p*C-a/P@200 may still contain a portion of arylamine Mannich structures, since the tri-substituted benzene ring absorption band at 1502 cm^{-1} didn't disappear completely.

3.5. Thermal stability of polybenzoxazines with different chemical structures

The thermal stability of polybenzoxazines consisted of different chemical structures was probed and the results are shown in Fig. 7 and Table 3. As expected, the N,O-acetal type polybenzoxazine (*p*C-a/P@30) showed the lowest T_{d5} (93 °C) and Y_c at 800 °C (23.7%); the arylamine Mannich type polybenzoxazine (*p*C-a/P@100 and *p*C-a/P@150) showed moderate T_{d5} and Y_c while the phenolic Mannich type polybenzoxazine (P*p*C-a@200) prepared without catalyst showed high thermal stability with T_{d5} of 274 °C and Y_c of 28.3%. Interestingly, *p*C-a/P@200 possessed the highest thermal stability, with T_{d5} at 290 °C and Y_c of 32.5%. The highest thermal stability of *p*C-a/P@200 may be caused by three reasons: (1) the thermally unstable iminium ions dissociated or further reacted at 200 °C as revealed by FTIR and ^{1}H NMR spectra, which decreased the proportion of weak moieties and improved T_{d5} and Y_c; (2) more phenolic Mannich and phenolic structures were formed, which increased the content of thermally more stable moieties; (3) the

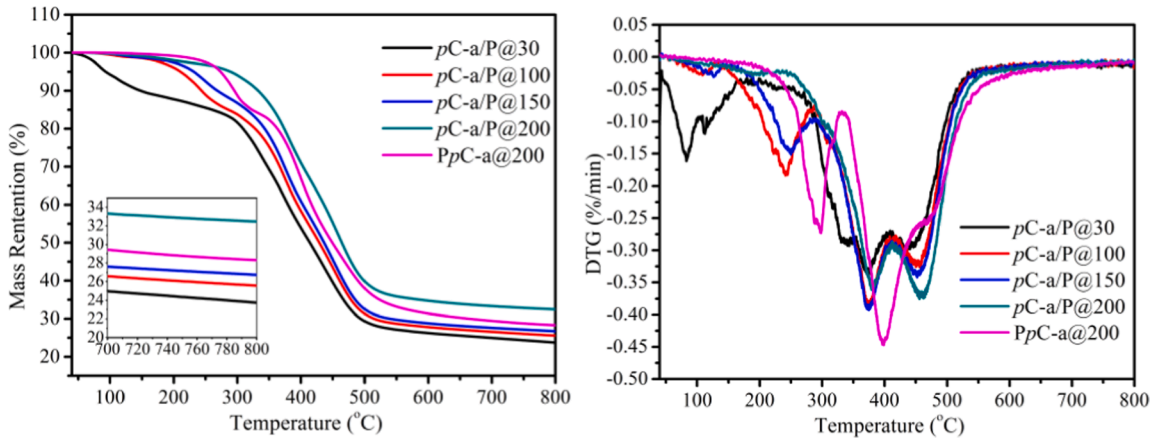

Fig. 7. TGA and DTG thermograms of poly(*p*C-a)s consisted of different chemical structures.

Table 3
TGA test results of poly(*p*C-a)s consisted of different chemical structures.

Sample	T_{d5} (°C)	T_{d10} (°C)	Y_c (800 °C, %)
*p*C-a/P@30	93	148	23.7
*p*C-a/P@100	211	244	25.6
*p*C-a/P@150	231	269	26.7
*p*C-a/P@200	290	333	32.5
P*p*C-a@200	274	295	28.3

arylamine Mannich structures in *p*C-a/P@200 anchored the dangling benzene rings and reduced the loss of aniline moieties.

Much more information can be interpreted from the DTG thermograms and used to facilitate verifying the previous discussions. For a typical aniline-based phenolic Mannich type polybenzoxazine, the aniline moieties are decomposed prior to phenolic moieties [41,49]. For P*p*C-a@200, as shown in the DTG thermograms in Fig. 7, the aniline moieties were extensively dissociated at around 300 °C and the phenolic moieties were massively decomposed at around 400 °C. Nevertheless, the decomposition peak for the aniline moieties was not observed for *p*C-a/P@200 because the aniline moieties were anchored by the arylamine Mannich structures. Moreover, as a result of the less-anchored phenolic moieties, the decomposition temperature for phenolic moieties slightly decreased to around 380 °C. As for the typical arylamine Mannich type polybenzoxazines *p*C-a/P@100 and *p*C-a/P@150, the decomposition peaks at around 250 °C may be mainly caused by the loss of thermally

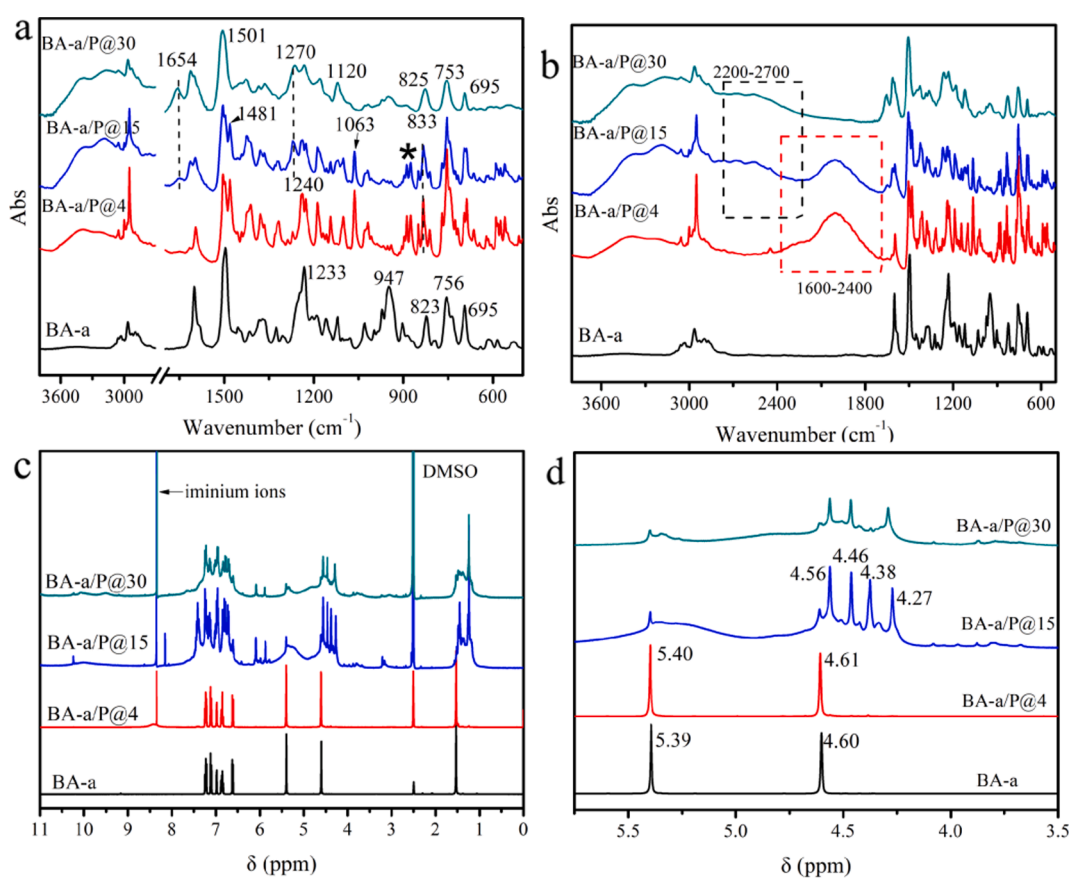

Fig. 8. FTIR spectra (a, b) and ^{1}H NMR spectra (c, d) of poly(BA-a)s catalyzed by PCl_5 in DCM at 4, 15 and 30 °C.

unstable iminium ions. The N,O-acetal type polybenzoxazine, *p*C-a/P@30, showed a decomposition peak below 100 °C, which was believed to be caused by the dissociation of weak phenoxyl bonds and loss of aniline moieties. Additionally, the evaporation of some residual solvent may also contribute to the phenomenon. To sum up, the results from the TGA tests well confirmed the proposed chemical structures of the polybenzoxazines.

3.6. N,O-acetal Polybenzoxazines prepared by catalytic ROP of BA-a in DCM

On the basis of previous understanding about catalytic ROP of benzoxazine, the bifunctional benzoxazine monomer, BA-a, was employed to synthesize N,O-acetal polybenzoxazine so as to evaluate its properties. In order to obtain N,O-acetal polybenzoxazine, low-polarity solvent DCM and relatively low temperatures of 4, 15 and 30 °C were utilized. Though the difference of the temperature was minor, the appearance of the products was quite different; BA-a/P@4 and BA-a/P@15 formed compact and crispy white films while BA-a/P@30 was fluffy yellow powder (Fig. S2). Spectroscopic characterizations were performed to figure out the chemical structures of the polybenzoxazines. As can be seen in Fig. 8a and b, the FTIR spectra of BA-a/P@4 and BA-a/P@30 were quite different while BA-a/P@15 showed some combined features of both BA-a/P@4 and BA-a/P@30. For BA-a/P@4, several structurally related features should be noted: (1) the characteristic band of the benzoxazine ring attributed to either a —C—O—C- cyclic acetal vibrational mode or a C—H out-of-plane deformation at 947 cm^{-1} disappeared, suggesting the ring-opening of the oxazine rings; (2) a pair of ether bond-related bands showed up at 1240 and 1063 cm^{-1}, which was the typical feature of N,O-acetal structures in polybenzoxazines as the previous study demonstrated [48]; (3) a new band emerged at 888 cm^{-1} (indicated by a black asterisk), which may be attributed to the Ar—H stretching mode of tri-substituted benzene rings; although tri-substituted benzene rings existed in BA-a, the bond strength and chemical environment probably changed due to ring-opening and formation of N,O-acetal structures, thus a new band was shown; (4) a weak phenolic hydroxyl-related band was shown at around 3400 cm^{-1}, suggesting the generation of a small portion of phenolic hydroxyls. Overall, it was believed that BA-a/P@4 was a N,O-acetal type polybenzoxazine as the previous features suggested.

For BA-a/P@30, some different results were found: (1) the intensity of the phenolic hydroxyl-related absorption band at around 3167 $cm^{-1}$was much higher than that of the BA-a/P@4; (2) the ether bond (Ar—O—C in N,O-acetal structures) absorption band at 1063 cm^{-1} disappeared completely while a new absorption band which may be attributed to phenolic Ar—O stretching emerged at 1270 cm^{-1}. Moreover, the Ar—H stretching absorption band of tri-substituted benzene ring at 888 cm^{-1} also disappeared completely. These results combined suggested the disapperance of the N,O-acetal structures; (3) the intensity of mono-substituted benzene ring absorption band (Ar—H stretching) at 753 cm^{-1} and 695 cm^{-1} decreased obviously while the intensity of tri-substituted benzene ring absorption band (C═C stretching) at 1501 cm^{-1} hardly changed, hence it is speculated that BA-a/P@30 was mainly composed of arylamine Mannich structures; (4) the absorption band of iminium ions became stronger as the temperature rose, which was caused by the dissociation of the N,O-acetal structures or the formation of more active intermediates.

A very interesting phenomenon was shown in Fig. 8b, that was, a broad band in the range of 1600–2400 cm^{-1} was observed in the FTIR spectra of both BA-a/P@4 and BA-a/P@15 while another band in the range of 2200–2700 cm^{-1} was seen in the FTIR spectra of both BA-a/P@15 and BA-a/P@30. Referring to the previous studies [47,48], we attributed these two bands to two different types of ammonium salts. Specifically, the band in the range of 2200–2700 cm^{-1} was assigned to the ammonium salt formed in the arylamine Mannich structure (Type I in Scheme 7) while the band in the range of 1600–2400 cm^{-1} was attributed to ammonium salt formed in N,O-acetal structure (Type II in Scheme 7). The variation of these two bands reflected the chemical structure evolution of the polybenzoxazines, from the N,O-acetal structures to the arylamine Mannich structures with elevated temperature.

The ^{1}H NMR spectra in Fig. 8c and d further corroborated the previous inferences. Firstly, very strong signals of the proton in phenolic hydroxyls and iminium ions were observed in 10.03 ppm and 8.32 ppm, respectively, for BA-a/P@15 and BA-a/P@30, manifesting the formation of massive phenolic hydroxyls and iminium ions at relatively high temperatures. Secondly, as Fig. 8d shows, it's interesting to find out that the signals of CH_2 protons in N,O-acetal type polybenzoxazine (BA-a/P@4) emerged at 5.40 ppm and 4.61 ppm, which were quite close to those of BA-a. Nevertheless, as the reaction temperature rose, the N,O-acetal structures transformed into other chemical structures, the signals at 5.40 ppm and 4.61 ppm weakened obviously and new signals

Table 4
SEC test results of poly(BA-a)s catalyzed by PCl_5 in DCM at different temperature for 24 h.

Sample	*Mn* (Dalton)	*Mw* (Dalton)	PDI
BA-a	989	1031	1.04
BA-a/P@4	7651	8511	1.11
BA-a/P@15	8127	9136	1.12
BA-a/P@30	8450	10,056	1.19

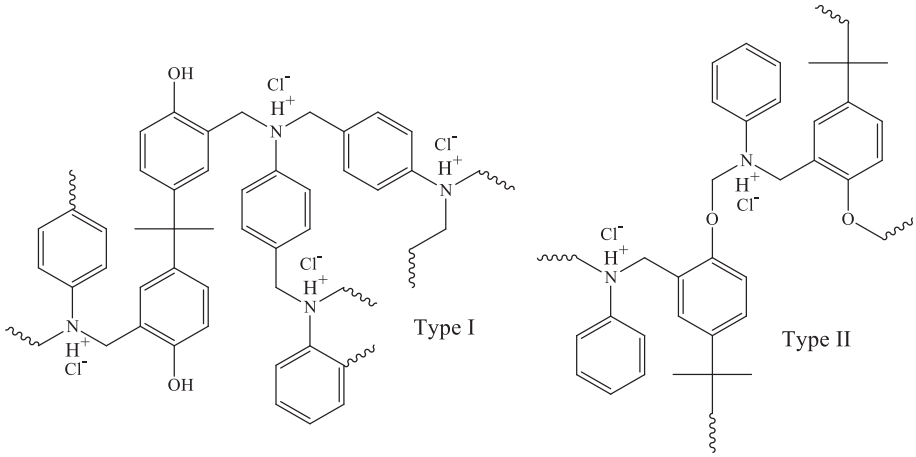

Scheme 7. Proposed chemical structures of ammonium salts in different polybenzoxazines.

attributed to arylamine Mannich methylene proton appeared in the range of 4.00–4.50 ppm. Furthermore, as the SEC test results in Table 4 and Fig. S7 revealed, the molecular weight and PDI increased slightly as the reaction temperature rose.

It is interesting to note that N,O-acetal type polybenzoxazine with high purity can not be obtained from *p*C-a while the N,O-acetal type polybenzoxazine BA-a/P@4 can be obtained. It is believed that the different chain moveability, steric effect and reaction time of the two monomers may be the main factors. That is, the steric hindrance of monofunctional *p*C-a is lower than bifunctional BA-a, and poly(*p*C-a) shows better chain moveability, thus chemical structure rearrangement of poly(*p*C-a) is easier. Moreover, the reaction time of poly(*p*C-a) is longer, which provides enough time for poly(*p*C-a) to rearrange. Comparatively, BA-a/P@4 precipitated after reaction for about 2 h, which would impede chemical structure rearrangement.

The thermal stability of BA-a/P@4, BA-a/P@30 and PBA-a@200 was characterized and the results are shown in Fig. 9 and Table 5. Resembling the N,O-acetal type polybenzoxazine synthesized from monofunctional benzoxazine monomer (*p*C-a/P@30), BA-a/P@4 showed a low T_{d5} (121 °C) and Y_c at 800 °C (17.0%). As the DTG thermogram of BA-a/P@4 presents, the phenoxyl bonds massively decomposed at around 140 °C; the aniline moieties decomposed at around 200 °C and the phenolic moieties decomposed at around 300 °C, which was caused by low bond energy and low crosslinking density. By contrast, the phenolic Mannich type polybenzoxazine PBA-a@200 possessed a high T_{d5} of 324 °C a high Y_c of 28.0%. It's noteworthy that BA-a/P@30 possessed relatively a low T_{d5} of 159 °C but the highest Y_c of 30.3%. Such a phenomenon may be caused by the decomposition of weak iminium ions at relatively low temperature but anchoring of dangling aniline moieties. In the DTG thermogram of BA-a/P@30, the decomposition peak at 230 °C may be due to the iminium ions; nevertheless, the decomposition rate of aniline moieties drastically decreased. Therefore, anchoring the dangling aniline moieties and eliminating the generation of iminium ions should beneficial to high thermal stability.

It is interesting to note that when compared with the Ref. [48], the FTIR spectrum of the polyBA-a initiated by PCl_5 in Ref. [48] is similar to that of BA-a/P@30. However, the T_g and thermal stability of sample obtained in Ref. [48] are much higher than those of BA-a/P@30. It is speculated that the much higher thermal properties may be caused by the post-treatment at 100 °C for 2 h, which was intended to get rid of solvent. The polyBA-a synthesized in organic solvent by catalytic ROP is thermally unstable and may transform into polybenzoxazine with other chemical structures, as indicated by the DSC thermograms in Fig. 9 of Ref. [48] and Fig. S8 of this work. Moreover, the trichloromethane used in Ref. [48] may also contribute to the better thermal properties.

The relationship between synthesis conditions, polymerization routes, chemical structures and thermal properties is established based on previous studies. Further, we proposed the underlying mechanisms behind the phenomena (Fig. 10). (1) In terms of catalyst, as a strong Lewis acid, PCl_5 coordinates with electron-rich sites such as oxygen atoms. Consequently, the C-O bonds in the oxazine rings are weakened and then dissociated to give reactive intermediates, which is the reason why ROP can take place at very low temperatures. Moreover, the electrons in *ortho*-position of C-O bonds are reduced due to inductive effect, making it hard for electrophilic attack to happen. Comparatively, the electron-rich oxygen atoms, ortho and para positions of aniline moieties are more favorable reaction sites and N,O-acetal structures and arylamine Mannich structures can be given, respectively, after electrophilic attack. (2) As for solvents, the relative dielectric constant of DCM at room temperature is 9, while that of DMF is 38, which reflects the huge polarity differences between the two solvents. Obviously, the polarity of N,O-acetal structures is lower than that of the arylamine Mannich structures because the polarity of ether bonds is lower than that of the phenolic hydroxyls. Therefore, N,O-acetal and phenoxyl structures are unstable in DMF due to the huge polarity difference and they tend to rearrange into arylamine Mannich structures, as previous study shows. (3) From the thermodynamic point of view, the oxygen and nitrogen atoms are more electronegative than the ortho and para positions of aniline benzene rings, thus the carbocations attack the oxygen and nitrogen atoms preferentially. Therefore, N,O-acetal and phenoxyl structures are more likely to be formed at low temperature and in the early stage of the ROP. Comparatively, the activation energy of electrophilic reaction on aniline benzene rings is higher and the reaction needs higher temperature to proceed. Additionally, the arylamine Mannich structures are thermally more stable, and they will not transform into N,O-acetal and phenoxyl structures once they are formed. Therefore, arylamine Mannich structures can be obtained upon raising the temperature and prolonging the reaction time.

Table 5
TGA test results of poly(BA-a)s consisted of different chemical structures.

Sample	T_{d5} (°C)	T_{d10} (°C)	Y_c (800 °C, %)
PBA-a200	324	348	28.0
BA-a/P@4	121	154	17.0
BA-a/P@30	159	201	30.3

4. Conclusions

The chemical structures of the polybenzoxazines synthesized under different reaction conditions were analyzed systematically and comprehensively. The relationship between synthesis conditions, polymerization mechanisms, chemical structures and thermal properties is established. Specifically, synthesis of polybenzoxazines consisted of N,O-acetal structures and phenoxy structures requires low-polarity solvent, relatively low temperature (-20 °C) and highly active catalyst PCl_5; preparation of polybenzoxazines composed of arylamine Mannich structures demands polar solvent and relatively high temperature in the

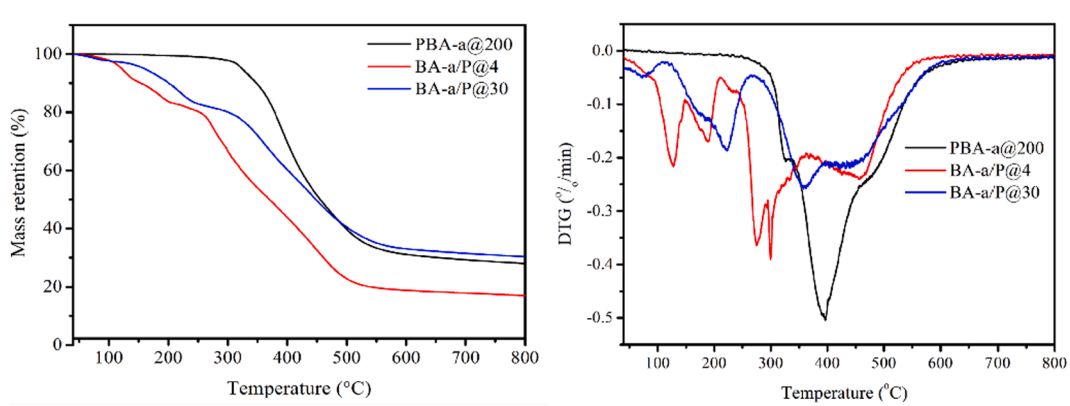

Fig. 9. TGA and DTG thermograms of poly(BA-a)s consisted of different chemical structures.

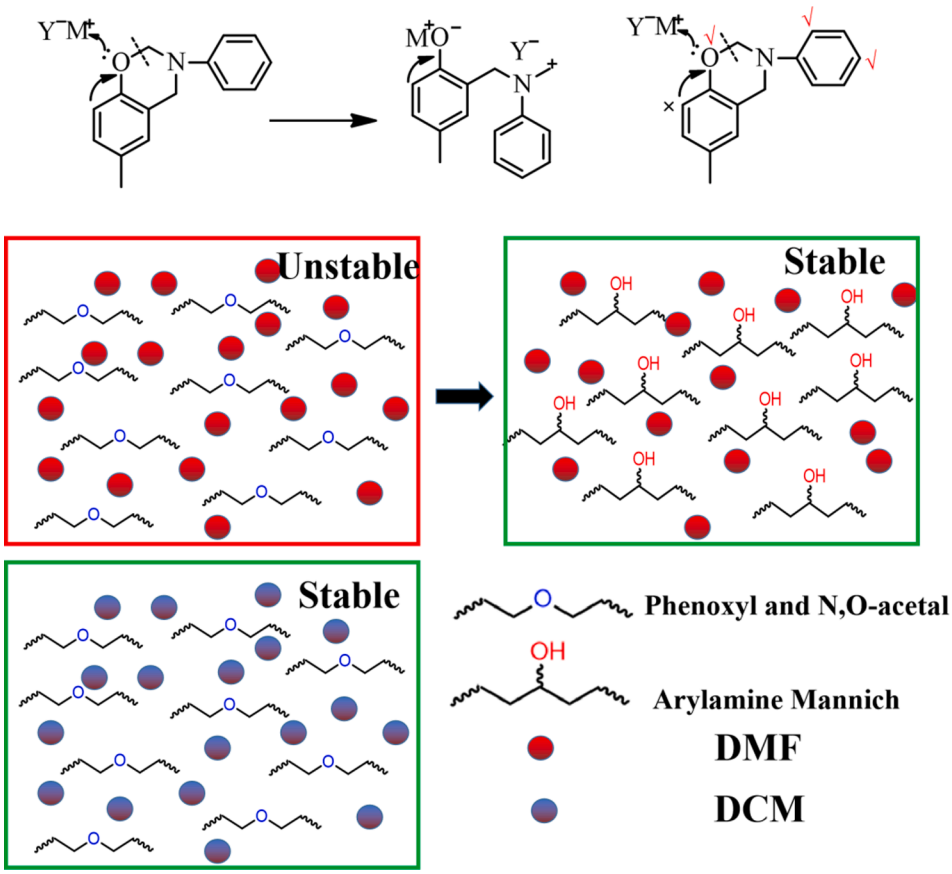

Fig. 10. Schematic description of influences of catalyst and solvents.

presence of PCl_5. Nevertheless, polybenzoxazines with phenolic Mannich structures can be obtained at high temperature (>180 °C) without any catalysts. In terms of thermal properties, the phenoxy structures are the most unstable structures, which will rearrange into N,O-acetal structures and arylamine Mannich structures upon prolonging reaction time or elevating temperature, thus N,O-acetal type polybenzoxazines show the lowest T_{d5} and Y_c. The arylamine Mannich structures could rearrange into phenolic Mannich and phenolic methylene structures at elevated temperature, but the arylamine Mannich type polybenzoxazines possess the highest char yield because of the anchoring of the dangling aniline moieties. The findings in this work are believed to provide more guidance for approaches to tailoring the properties of the polybenzoxazines.

Declaration of Competing Interest

The authors declare that they have no known competing financial interests or personal relationships that could have appeared to influence the work reported in this paper.

Acknowledgement

This work is supported by the National Natural Science Foundation of China (Project No. 21104048 and No. 52073188).

Declaration of Competing Interest

The authors declare no competing financial interest.

Data Availability

The raw/processed data required to reproduce these findings cannot be shared at this time as the data also forms part of an ongoing study.

Appendix A. Supplementary material

Supplementary data to this article can be found online at https://doi.org/10.1016/j.eurpolymj.2020.110133.

References

[1] C.P.R. Nair, Advances in addition-cure phenolic resins, Prog. Polym. Sci. 29 (5) (2004) 401–498.
[2] T. Takeichi, T. Agag, High performance polybenzoxazines as novel thermosets, High Perform. Polym. 18 (2006) 777–797.
[3] N.N. Ghosh, B. Kiskan, Y. Yagci, Polybenzoxazines—New high performance thermosetting resins: Synthesis and properties, Prog. Polym. Sci. 32 (11) (2007) 1344–1391.
[4] H. Ishida, Chapter 1 - overview and historical background of polybenzoxazine research, in: H. Ishida, T. Agag (Eds.), Handbook of Benzoxazine Resins, Elsevier, Amsterdam, 2011, pp. 3–81.
[5] B. Kiskan, Adapting benzoxazine chemistry for unconventional applications, React. Funct. Polym. 129 (2018) 76–88.
[6] Y. Lyu, H. Ishida, Natural-sourced benzoxazine resins, homopolymers, blends and composites: A review of their synthesis, manufacturing and applications, Prog. Polym. Sci. 99 (2019) 101168.
[7] P. Pattharasiriwong, C. Jubsilp, P. Mora, S. Rimdusit, Dielectric and thermal behaviors of fluorine-containing dianhydride-modified polybenzoxazine: A molecular design flexibility, J. Appl. Polym. Sci. 134 (33) (2017).
[8] G.A. Phalak, D.M. Patil, S. Mhaske, Synthesis and characterization of thermally curable guaiacol based poly (benzoxazine-urethane) coating for corrosion protection on mild steel, Eur. Polym. J. 88 (2017) 93–108.
[9] Y. Xu, J. Dai, Q. Ran, Y. Gu, Greatly improved thermal properties of polybenzoxazine via modification by acetylene/aldehyde groups, Polymer 123 (2017) 232–239.
[10] Y. He, S. Gao, Z. Lu, A mussel-inspired polybenzoxazine containing catechol groups, Polymer 158 (2018) 53–58.
[11] K. Zhang, X. Yu, S.-W. Kuo, Outstanding dielectric and thermal properties of main chain-type poly(benzoxazine-co-imide-co-siloxane)-based cross-linked networks, Polym. Chem. 10 (19) (2019) 2387–2396.

[12] K. Zhang, Y. Liu, M. Han, P. Froimowicz, Smart and sustainable design of latent catalyst-containing benzoxazine-bio-resins and application studies, Green Chem. 22 (4) (2020) 1209–1219.
[13] S. Rimdusit, M. Lohwerathama, K. Hemvichian, P. Kasemsiri, I. Dueramae, Shape memory polymers from benzoxazine-modified epoxy, Smart Mater. Struct. 22 (7) (2013) 075033.
[14] S. Zhang, Q. Ran, Q. Fu, Y. Gu, Preparation of transparent and flexible shape memory polybenzoxazine film through chemical structure manipulation and hydrogen bonding control, Macromolecules 51 (17) (2018) 6561–6570.
[15] O.S. Taskin, B. Kiskan, Y. Yagci, Polybenzoxazine precursors as self-healing agents for polysulfones, Macromolecules 46 (22) (2013) 8773–8778.
[16] P. Sharma, S. Shukla, B. Lochab, D. Kumar, P. Kumar Roy, Microencapsulated cardanol derived benzoxazines for self-healing applications, Mater. Lett. 133 (2014) 266–268.
[17] L. Wan, J. Wang, L. Xie, Y. Sun, K. Li, Nitrogen-enriched hierarchically porous carbons prepared from polybenzoxazine for high-performance supercapacitors, ACS Appl. Mater. Interfaces 6 (17) (2014) 15583–15596.
[18] A.A. Alhwaige, H. Ishida, S. Qutubuddin, Carbon aerogels with excellent CO2 adsorption capacity synthesized from clay-reinforced biobased chitosan-polybenzoxazine nanocomposites, ACS Sustainable Chem. Eng. 4 (3) (2016) 1286–1295.
[19] J.-Y. Wu, M.G. Mohamed, S.-W. Kuo, Directly synthesized nitrogen-doped microporous carbons from polybenzoxazine resins for carbon dioxide capture, Polym. Chem. 8 (36) (2017) 5481–5489.
[20] C. Wang, J. Sun, X. Liu, A. Sudo, T. Endo, Synthesis and copolymerization of fully bio-based benzoxazines from guaiacol, furfurylamine and stearylamine, Green Chem. 14 (10) (2012) 2799–2806.
[21] B.S. Rao, A. Palanisamy, Monofunctional benzoxazine from cardanol for bio-composite applications, React. Funct. Polym. 71 (2) (2011) 148–154.
[22] X.-Y. He, J. Wang, Y.-D. Wang, C.-J. Liu, W.-B. Liu, L. Yang, Synthesis, thermal properties and curing kinetics of fluorene diamine-based benzoxazine containing ester groups, Eur. Polym. J. 49 (9) (2013) 2759–2768.
[23] G. Lligadas, A. Tüzün, J.C. Ronda, M. Galià, V. Cádiz, Polybenzoxazines: new players in the bio-based polymer arena, Polym. Chem. 5 (23) (2014) 6636–6644.
[24] K. Zhang, M. Han, Y. Liu, P. Froimowicz, Design and synthesis of bio-based high-performance trioxazine benzoxazine resin via natural renewable resources, ACS Sustainable Chem. Eng. 7 (10) (2019) 9399–9407.
[25] H. Kimura, A. Matsumoto, K. Ohtsuka, Studies on new type of phenolic resin—Curing reaction of bisphenol-A-based benzoxazine with epoxy resin using latent curing agent and the properties of the cured resin, J. Appl. Polym. Sci. 109 (2) (2008) 1248–1256.
[26] H. Wang, Z. Pei, L. Hong, Q. Ran, G. Yi, The effect of curing cycles on curing reactions and properties of a ternary system based on benzoxazine, epoxy resin, and imidazole, J. Appl. Polym. Sci. 127 (3) (2013) 2169–2175.
[27] R.-C. Lin, M.G. Mohamed, T. Chen, S.-W. Kuo, Coumarin-and carboxyl-functionalized supramolecular polybenzoxazines form miscible blends with polyvinylpyrrolidone, Polymers 9 (4) (2017) 146.
[28] A. Sudo, H. Yamashita, T. Endo, Ring-opening polymerization of 1,3-benzoxazines by p-toluenesulfonates as thermally latent initiators, J. Polym. Sci., Part A: Polym. Chem. 49 (16) (2011) 3631–3636.
[29] A. Ručigaj, B. Alič, M. Krajnc, U. Šebenik, Curing of bisphenol A-aniline based benzoxazine using phenolic, amino and mercapto accelerators, eXPRESS Polym. Lett. 9 (7) (2015).
[30] A. Kocaarslan, B. Kiskan, Y. Yagci, Ammonium salt catalyzed ring-opening polymerization of 1, 3-benzoxazines, Polymer 122 (2017) 340–346.
[31] T. Urbaniak, M. Soto, M. Liebeke, K. Koschek, Insight into the mechanism of reversible ring-opening of 1, 3-benzoxazine with thiols, J. Organic Chem. 82 (8) (2017) 4050–4055.
[32] Q.C. Ran, N. Gao, Y. Gu, Thermal stability of polybenzoxazines with lanthanum chloride and their crosslinked structures, Polym. Degrad. Stab. 96 (9) (2011) 1610–1615.
[33] Yongfei Zhu, Yi Gu, Effect of interaction between transition metal oxides and nitrogen atoms on thermal stability of polybenzoxazine, J. Macromol. Sci. Part B 50 (6) (2011) 1130–1143.
[34] Y. Zhu, L. Hong, G. Yi, Effect of LaO on the thermal stability of polybenzoxazine based on 4,4′-diaminodiphenyl methane, J. Polym. Res. 19 (7) (2012), 9904–684.
[35] P. Chutayothin, H. Ishida, Cationic ring-opening polymerization of 1,3-benzoxazines: mechanistic study using model compounds, Macromolecules 43 (10) (2010) 4562–4572.
[36] S. Zhang, J. Zong, Q. Ran, Y. Gu, Facile preparation of lightweight and robust polybenzoxazine foams, Ind. Eng. Chem. Res. 59 (16) (2020) 7575–7583.
[37] Q.-C. Ran, D.-X. Zhang, R.-Q. Zhu, Y. Gu, The structural transformation during polymerization of benzoxazine/FeCl3 and the effect on the thermal stability, Polymer 53 (19) (2012) 4119–4127.
[38] X. Ning, H. Ishida, Phenolic materials via ring-opening polymerization: Synthesis and characterization of Bisphenol A based benzoxazine and their polymers, J. Polym. Sci., Part A: Polym. Chem. 32 (6) (1994) 1121–1129.
[39] Y. Bai, P. Yang, Y. Song, R. Zhu, Y. Gu, Effect of hydrogen bonds on the polymerization of benzoxazines: influence and control, RSC Adv. 6 (51) (2016) 45630–45635.
[40] J. Dunkers, H. Ishida, Vibrational assignments of N, N-bis(3,5-dimethyl-2-hydroxybenzyl)methylamine in the fingerprint region, Spectrochim. Acta Part A Mol. Biomol. Spectrosc. 51 (5) (1995) 855–867.
[41] S. Zhang, Q. Ran, Q. Fu, Y. Gu, Controlled polymerization of 3,4-dihydro-2H-1,3-benzoxazine and its properties tailored by Lewis acids, React. Funct. Polym. 139 (2019) 75–84.
[42] L. Han, D. Iguchi, P.S. Gil, T. Heyl, V.M. Sedwick, C.R. Arza, S. Ohashi, D.J. Lacks, H. Ishida, Oxazine ring-related vibrational modes of benzoxazine monomers using fully aromatically substituted, deuterated, (15)N isotope exchanged and oxazine-ring-substituted compounds and theoretical calculation, J. Phys. Chem. A 121 (33) (2017) 6269–6282.
[43] C. Liu, D. Shen, R.M. Sebastián, J. Marquet, R. Schönfeld, Mechanistic studies on ring-opening polymerization of benzoxazines: A mechanistically based catalyst design, Macromolecules 44 (12) (2011) 4616–4622.
[44] A. Sudo, R. Kudoh, H. Nakayama, K. Arima, T. Endo, Selective formation of poly(N, O-acetal) by polymerization of 1,3-benzoxazine and its main chain rearrangement, Macromolecules 41 (23) (2008) 9030–9034.
[45] L. Chao, D. Shen, R.M.A. SebastiáN, J. Marquet, R. SchöNfeld, Mechanistic studies on ring-opening polymerization of benzoxazines: A mechanistically based catalyst design, Macromolecules 44 (12) (2011) 4616–4622.
[46] Q.-C. Ran, D.-X. Zhang, R.-Q. Zhu, Y. Gu, The structural transformation during polymerization of benzoxazine/FeCl3 and the effect on the thermal stability, Polymer 53 (19) (2012) 4119–4127.
[47] Y.X. Wang, H. Ishida, Cationic ring-opening polymerization of benzoxazines, Polymer 40 (16) (1999) 4563–4570.
[48] Y.X. Wang, H. Ishida, Synthesis and properties of new thermoplastic polymers from substituted 3,4-Dihydro-2H-1,3-benzoxazines, Macromolecules 33 (8) (2000) 2839–2847.
[49] J.A. Macko, H. Ishida, Effects of phenolic substitution on the photooxidative degradation of polybenzoxazines, Macromol. Chem. Phys. 202 (11) (2001) 2351–2359.